Neural Representation of Spatial Location

CoMPLEX MRes Case Presentation 2

Elizabeth Gallagher
Supervisors: Neil Burgess, John OKeefe and Francesca Cacucci

March 7, 2013

Abstract

Place, boundary vector, head-direction and grid cells located in the hippocampus provide neural representations of space. This representation acts as a scaffold for learning about the environment, and develops independently of spatial experience. Investigating the properties of spatial firings in hippocampal cells from young animals may yield insights into how this scaffold emerges and develops.

Contents

1 Introduction

How we perceive our environment and our place in that environment has been questioned for centuries. Through the developments of neuroscience, Kant's argument that some of our spatial representation exists before environmental experience (as opposed to derivation from sensory impression alone) can be tested.

Investigation into whether or not the brain has an underlying cognitive map of location started with the work of Tolman (1948). The discovery of place cells (O'Keefe & Nadel, 1978) with spatially localised firings suggested that the hippocampus and its surrounding areas play a role in spatial representation. From there, the more recent discovery of grid cells in the medial entorhinal cortex by Hafting *et al* (2005) has suggested that an underlying metric for the estimation of location exists. Grid cells fire in a very regular pattern which could unfeasibly be because of individual association with features in the environment, and hence suggests that they act as a framework for the external spatial environment.

This cognitive map exists independently of exploration of the environment (O'Keefe & Nadel, 1978) and hence investigation into the firings properties of hippocampal cells in young animals could give us an insight into how this map emerges and develops.

This report will give a review of the methods used to obtain and analyse recordings of hippocampal cells. Data collected from rat pups between the ages of 16 and 30 days will be analysed. The number and the orientation of maximal Fourier components, as well as the percentage of spatially periodic cells will be found for each of the different ages.

2 Hippocampal Cells

The neuronal firing properties in the hippocampus of rodents have largely been the subject of experimentation when investigating spatial representation. This is done by recording the firing patterns of cells simultaneously with the animal's spatial location as it forages for food in a familiar enclosure. Cells are recorded from different sections of the hippocampus (see Figure 1 for locations), and different sections have a different composition of cell type.

Place, boundary vector, head-direction and grid cells have a temporal organisation known as theta phase precession. The interaction of these cells makes up the neural representation of space and self-location within the space (Burgess & O'Keefe, 2011).

2.1 Place, Boundary Vector and Head-direction Cells

Place cells are fired whenever the animal is in a specific region of the environment. This firing is independent of both the orientation of the animal and any external cues (Jeffery & Burgess, 2006). Figure 2a shows the firings of a place cell in relation to the location of the animal in an environment. Boundary vector cells fire whenever an environmental boundary is near to the animal (Lever *et al*, 2009) and fire independently of head-direction. These cells contribute environmental information to place cells, where place cell firing is a thresholded summation of the boundary vector cells which synapse into it.

Head-direction cells are fired when the animal is facing in a particular direction, independent of the animals location (Taube, 1998). These cells are thought to provide a sense of direction for spatial navigation.

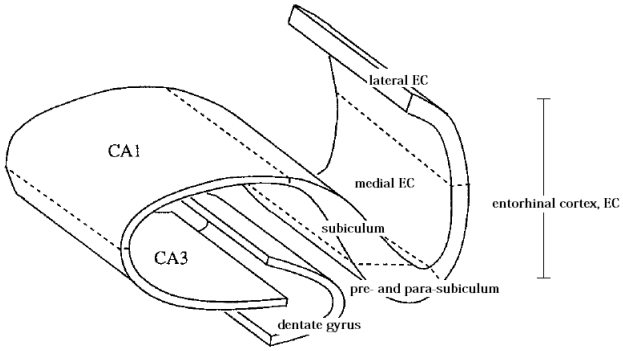

Figure 1: A schematic section cut perpendicular to the longitudinal axis of the hippocampus. Adapted from Burgess & O'Keefe (1996).

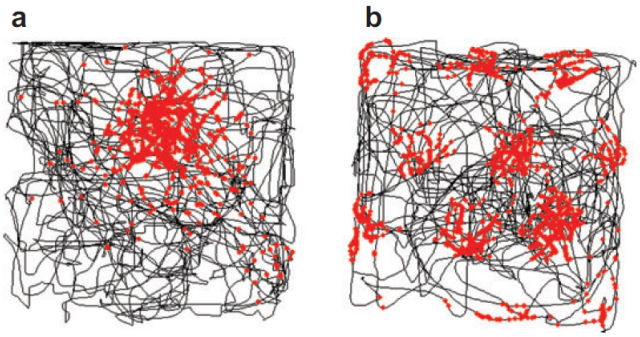

Figure 2: (a) Place cells in the hippocampus. (b) Grid cells in the medial entorhinal cortex. Spike locations in shown in red and the rats trajectory shown in black. Taken from Moser, Kropff & Moser (2008).

2.2 Grid cells

The spatial firings of grid cells form a periodic triangular arrangement (see Figure 2b). These cells are found in the medial entorhinal cortex (mEC) and pre- and parasubiculum, and have multiple spatial firing fields (Fyhn *et al*, 2004).

Different grid cells can be characterised by the spacing between their fields, the orientation relative to an external reference axis (the definition of orientation shown in Figure 3a) and their phase. Neighbouring grid cells in the mEC have a similar grid spacing and orientation (see Figure 3b), but their grid phase can be very different. Furthermore dorsally located cells have a smaller grid spacing than ventrally located cells (Figure 3b) (Hafting *et al*, 2005). Figure 3c illustrates how most of the environment explored by an animal is covered by the firings of different grid cells, with offset grids.

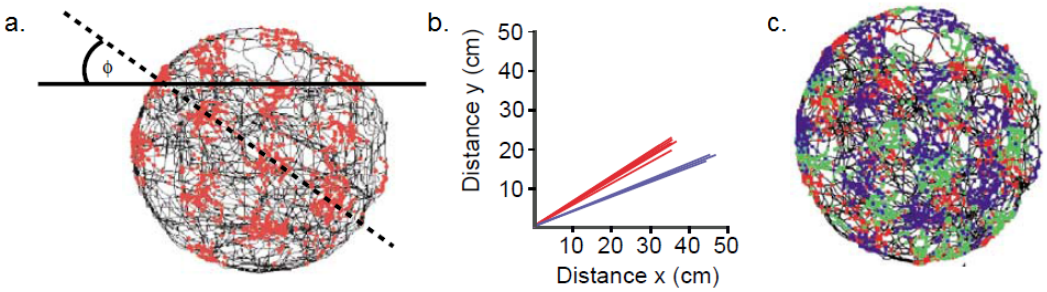

Figure 3: (a) The orientation of grids, Φ: the angle between a row of peaks and a camera-defined horizontal line. (b) Vector illustration of orientation; red lines show dorsally located cells, blue lines show ventrally located cells. (c) Superposition of three nearby grid cells' firing fields. Taken from Jeffery & Burgess (2006).

3 Analysis of Recordings

The firing rate of hippocampal cells (often from the superficial layers of the medial part of the dorsocaudal mEC and adjacent parasubiculum) are recorded simultaneously with the animals position as it moves around an environment. These cells are recorded by a microdrive implant loaded with four tetrodes. As there are multiple unit recordings from the tetrodes, single cells can be identified by manual cluster-cutting (see the supplementary materials for Krupic *et al* (2012) for details). The animal's position and direction are measured by tracking two LEDs which are fixed onto the animal.

The number of spikes fired in a section of the environment (2.5cm^2 bins in the case of Krupic *et al* (2012)) are divided by the time the rat spent there, and this information is used to produce an unsmoothed firing rate map. Smoothed rate maps are then found by applying a smoothing method (such as adaptive, boxcar or circular disc smoothing). Figure 4 shows the unsmoothed and smoothed rate map for a grid cell.

The spatial periodic firing patterns of the cells are made up of plane waves (bands) from a discrete set of orientations and wavelengths. Hence the firing pattern can be used to classify the type of cell being recorded.

3.1 2D Fourier Spectral Analysis

Cells which have a significant spatial periodicity in their spatial firing patterns can be identified by two-dimensional Fourier spectral analysis. The cells' spatial firing-rate is the summation of several Fourier components, which are periodic spatial bands with unique wavelengths and orientations.

The 2-D Fourier spectrogram can be calculated as:

$$F[l_y, l_x] = \frac{1}{fr_{mean}\sqrt{M_x N_y}} \sum_{n=0}^{N-1} \sum_{m=0}^{M-1} f[m,n] e^{-2\pi i \left(\frac{ml_y}{M} + \frac{nl_x}{N}\right)}, \quad (1)$$

where $f[m,n]$ is the unsmoothed firing rate map, with the mean firing rate subtracted and zero-padded (to increase spatial resolution) to have size $M_x \times N_y = 256 \times 256$. $F[l_y, l_x]$ is

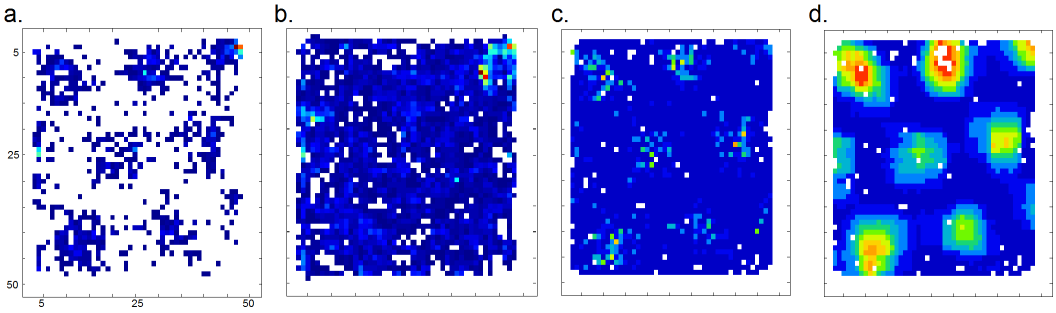

Figure 4: Representation of data from a grid cell (rat 1475, trial 091007d, tetrode 3, cell 1).a) Locations of spikes fired. b) Bins visited by rat. Unsmoothed (c) and boxcar smoothed (with kernel size 7) (d) rate maps. Low to high frequencies are shown in dark blue to dark red respectively, white represents no recordings from this bin.

a matrix of the Fourier components corresponding to unique plane waves specified by (l_y, l_x). fr_{mean} is the mean firing rate of the whole trial and M_x and N_y are the width and length of bins in the original firing rate map before zero-padding, dividing by $fr_{mean}\sqrt{M_x N_y}$ allows for comparison between firing rate maps from different sized environments and between cells with different firing rates.

3.2 Spatially Periodic Cells

If the cells' maximal Fourier component is higher than 95% of that in spatially shuffled data, then the cell can be classed as a spatially periodic cell (SPC) (see Figure 5a). The shuffled data is found by wrapping the time-shifted spike train around the position data. The maximum Fourier power, max$P[l_y, l_x]$, is:

$$P[l_y, l_x] = \sqrt{F^2_{real}[l_y, l_x] + F^2_{imag}[l_y, l_x]}. \quad (2)$$

Figure 5b shows the distribution of SPCs and the types of SPCs in the recordings from Krupic *et al* (2012).

Spatially periodic grid cells usually have three main Fourier components with similar wavelengths and with orientations at 60° from one another (see Figure 5c). Non-grid SPCs tend to have a greater range of relative orientations and wavelengths (Krupic *et al*, 2012).

3.3 Stability

The stability of the firing patterns in familiar environments, between successive trials on the same day and between successive trials on different days, can be considered. This stability is measured by calculating the Pearson product-moment correlation coefficient between the rate maps.

Krupic *et al* (2012) found that grid-cell firing patterns and the orientations of their Fourier components were more stable, on both comparisons, than those of spatially periodic non-grid cells.

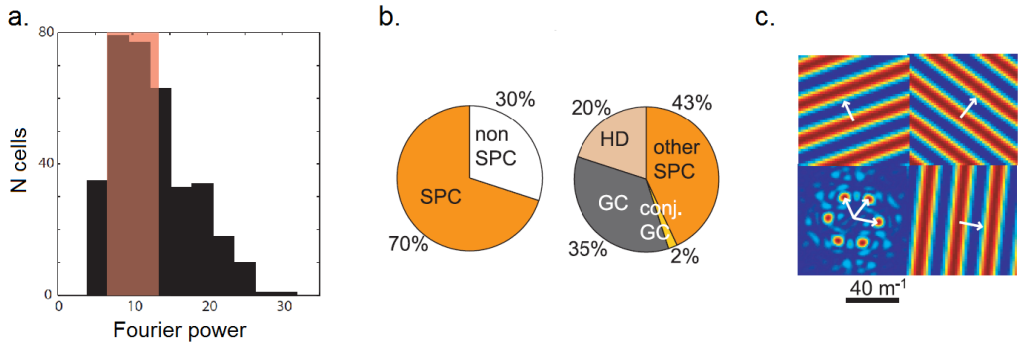

Figure 5: a) Histogram of maximum normalised Fourier power. The mean threshold ± standard deviation of 95th percentile values from shuffled data are shown in red. b) Composition of data from Krupic *et al* (2012). Proportion of spatially periodic cells (SPC) in all of the cells (left); proportional of grid cells (GC), conjunctive grid cells (conj. GC), head-direction correlates (HD) and others in the spatially periodic cells only (right). c) 2D Fourier spectrogram with wave vectors shown in white (bottom left) and the main Fourier components. Taken from Krupic *et al* (2012).

The stability across different environments can also be considered. From the recordings of Krupic *et al* (2012), 11% of the SPCs changed from grid cells to non-grid cells (or vice versa) between trials in the same environment, and 32% changed across different environments.

3.4 Orientation

From the analysis of Krupic *et al* (2012) the Fourier components of grid cells are aligned and orientated at 60° to one another. Furthermore, the orientations of spatially periodic non-grid cells are aligned with those of the grid cells, but also include other orientations (Figure 6a). Figures 6b & c show the distributions of the orientations of grid cells and of spatially periodic non-grid cells found. 65% of the cells in the mEC were spatially periodic, and of these 48% were grid cells. In the PaS 79% were spatially periodic, however here only 18% were grid cells.

It is suggested that the mEC's anatomical inputs prefer components at 60° and the parasubiculum might represent an intermediate stage in the construction of stable grids from periodic bands (Krupic *et al*, 2012).

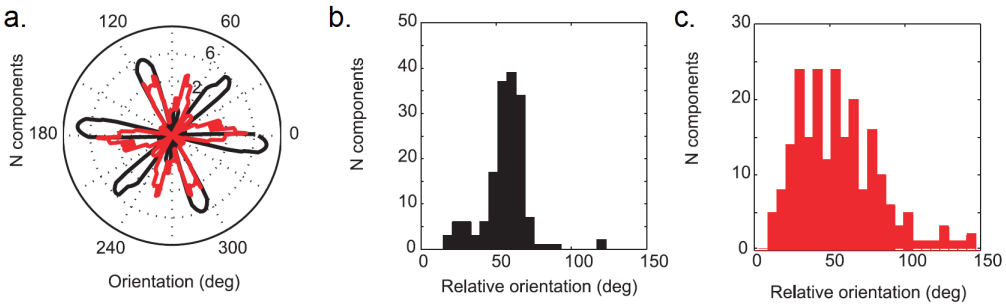

Figure 6: a) Histogram of the orientations of the main Fourier components of grid cells (black) and nongrid spatially periodic cells (red) in a single rat. Distributions of the relative orientations of the Fourier components of all the grid cells (b) and all the spatially periodic non-grid cells (c) from all rats analysed. Taken from Krupic *et al* (2012).

4 Spatial Representation with Age.

Hafting *et al* (2005) found that grid fields exist from the beginning of environmental exploration and furthermore prevail with landmark removal, but how much of a spatial map an animal is born with and how much is learnt from experience is unknown.

Anatomical development of the hippocampus continues up until rats are seven weeks old, and hence rats under P40 are impaired in spatial navigation tasks. In terms of specificity and stability of locational firing, it was found that place cell development progresses alongside spatial navigation development, but head-direction cells develop fully before hippocampus maturation (Martin & Berthoz, 2002).

Wills *et al* (2010) looked at the emergence and development of place, head-direction and grid cells when rat pups first began to explore their environment, which was typically at the age P16 (postnatal day 16). A similar pattern was found in several properties of these cells with age. The proportion of cells, their stability over time (measured from one trial to the next) and quality of spatial encoding (by using the spatial information per spike) were measured. It was found that both directional and place cells have significant adult-like amounts for these properties from P16 and in place cells they also increase with development. Significant amounts of grid cells, however, appear at P20 and level off at P22 (see Figure 7).

The data used for our analysis was taken from the recordings of hippocampal pyramidal cells and medial entorhinal cells from 42 male Lister Hooded rats between the ages of P16 and P30. Detailed information of the experimental procedure can be found in the supplementary material for Wills *et al* (2010). Cells were classed as grid cells if they had a gridness score (a definition of this can be found in the supplementary material of Krupic *et al* (2012)) of more than 0.3.

4.1 Cell Inclusion.

Of 2847 cell recordings, 1119 were selected for analysis. These satisfied the following conditions:

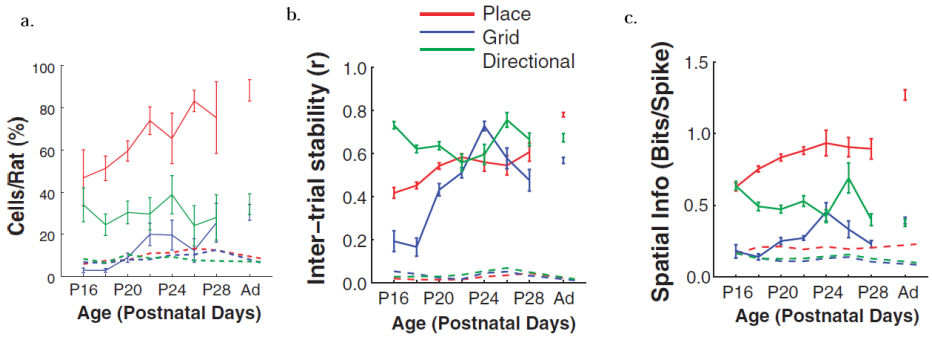

Figure 7: Patterns of three properties of directional (green), place (red) and grid (blue) cells with age. Mean percentage of cells per rat (a), stability (b) and quality of spatial encoding (c), as a function of age (solid lines). Dashed lines show the $p = 0.05$ significance level for the mean value for each cell type based on spike-shuffled data. Adapted from Wills *et al* (2010).

1. Spatial information, Rayleigh vector and gridness score have all been calculated;
2. the rat was recorded in a familiar environment;
3. the recording was probably taken from the EC1, EC2, EC3 or parasubiculum (each with certainty 2/3 or 3/3);
4. the length of the path taken by the rat was more than 45;
5. the number of spikes fired was more than 100;
6. the position data wasn't too sparse.

We found the percentage of bins that the rat had been in to find whether or not the position data was not too sparse. This was done by first trimming the position data and then calculating the percentage of visited bins in the trimmed environment, if this was over 80% the cell was included (see Figure 8).

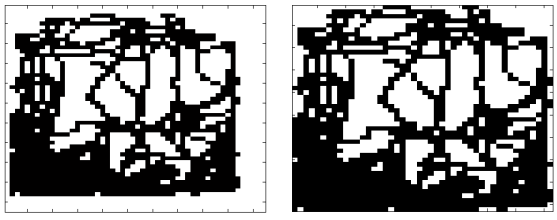

Figure 8: An example of trimming, before (left) and after (right). From the position data of trial 031007a, tetrode 3, cell 2. 56.57% of the trimmed environment has position data.

4.2 Reflections

Some of the data was corrupted by misinformation from reflections on the edge of the environment. This would cause the readings to falsely say that the rat had been in a position bin here. Hence, the position recordings were put through a filter to remove the false positions. If 80% or more of a row or column of bins were identified as 0 (i.e. the rat hadn't been there) then the whole row was converted to reading that the rat had not been there. This process was applied outwards in until the first row or column of less than 80% unvisited bins appears. Hence if there was a row or column in the centre of the environment where the rat happens to never visit, it would not be converted to a row or column of unvisited bins. Figures 9a & b show this filtering process.

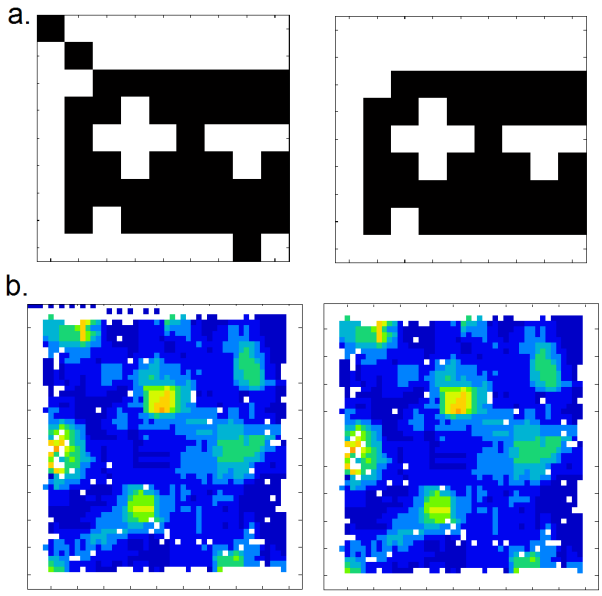

Figure 9: Reflection filtering. a) Illustration of how reflection filtering works, before (left) and after (right). Row 5 and column 4 remain unchanged even though they have more than 80% unvisited bins. b) Smoothed rate map for 121107g, tetrode 2, cell 2. Before (left) and after (right) the application of reflection filtering.

4.3 Fourier Components

The Fourier power spectrum was found for each cell. It was normalised to be between 0 and 1 for ease of comparison. Figure 14 shows the Fourier power plots for ten rats with ages separately coloured. The mean Fourier power for both grid and non-grid cells per age for each rat were also found (Figures 15 and 16).

The maximum Fourier components were found for each cell, this was done by a process of smoothing the power spectrum and then finding maxima (this process can be seen in Figure 10). The distribution of the angles of the maximum components follows a general pattern in both the grid and non-grid cells (see Figure 11), with peaks at around 10°, 90°

and 170° in both. There was not much diversion from this trend when looking at ages separately either (see Figures 17 and 18).

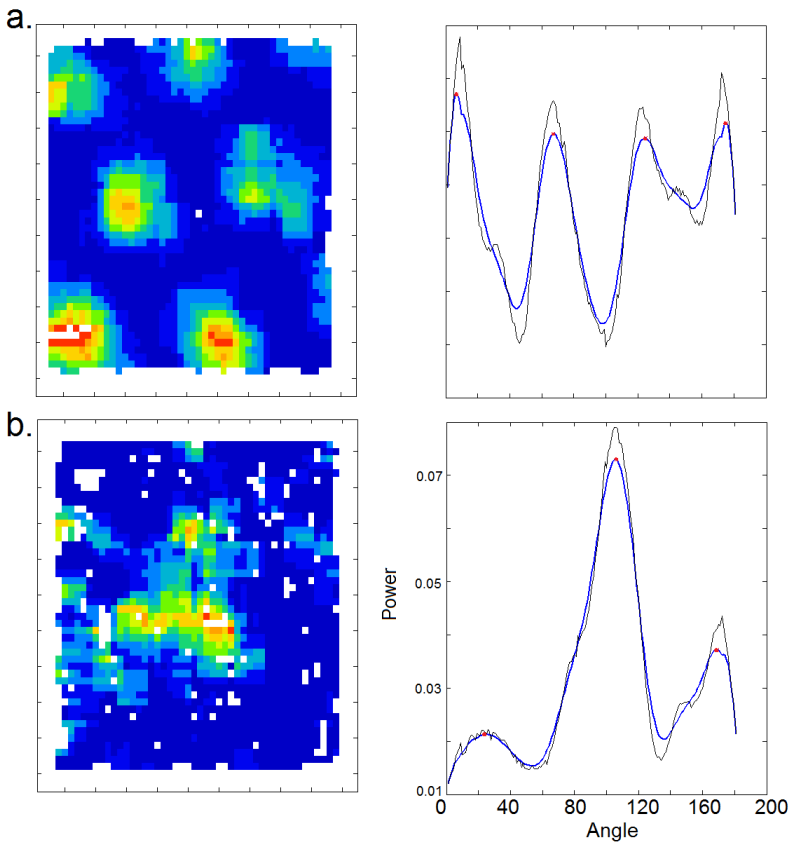

Figure 10: Examples of finding maxima for a grid (rat 1475, trial 081007a, tet 3, cell 1) (a) and non-grid cell (rat 1514, trial 071207e, tet 2, cell 2) (b). Smoothed rate maps shown on left and Fourier power shown on right. Fourier power (black), Fourier power smoothed (blue), maximum peaks (minimum distance between peaks taken as 20) (red points).

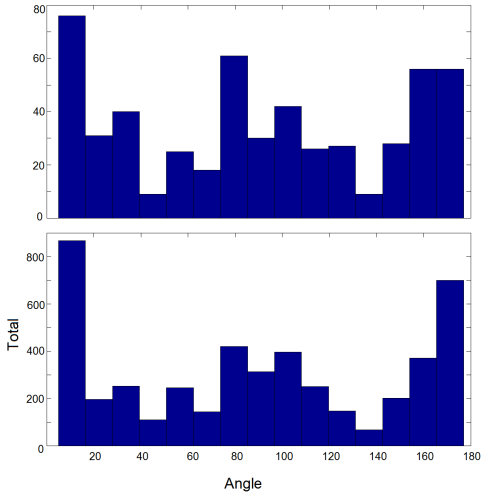

Figure 11: Distribution of maximum Fourier components of grid (above) and non-grid (below) cells

4.4 Spatially Periodic Cells

The spike data was shuffled 1000 times and the maximum Fourier component was taken each time. The 95^{th} percentile was found for these 1000 maximum Fourier components. Cells were classed as spatially periodic if their maximum Fourier power was over this percentile. Of the cells analysed, 18% were classed as spatially periodic. 43% of grid cells were classed as spatially periodic and 14% of non-grid cells were classed as spatially periodic. The percentage of cells which were spatially periodic increased with age (see Figure 12). In non-grid cells the number which were spatially periodic didn't change much with age, however in grid cells the number seemed to increase with age (see Figure 13).

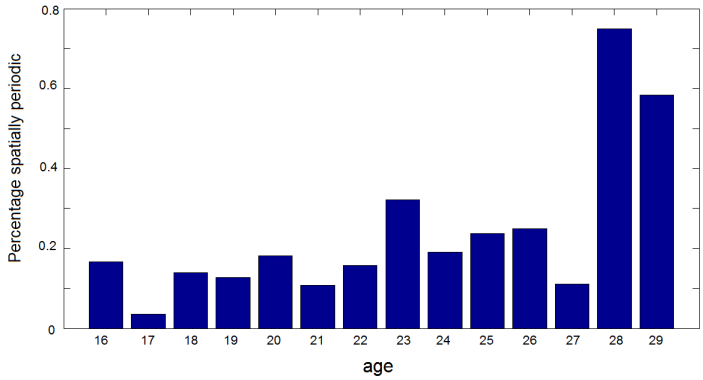

Figure 12: Percentage of SPCs for each age.

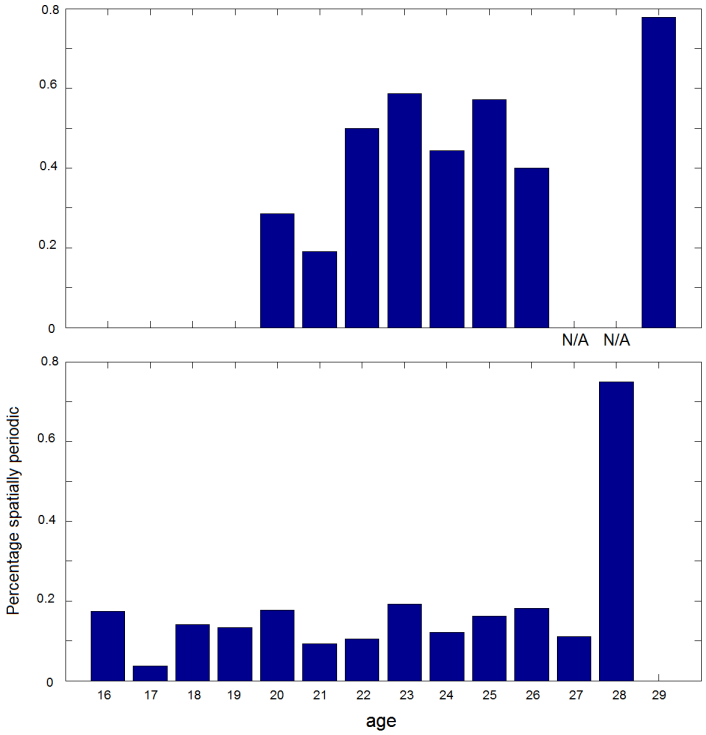

Figure 13: Percentage of SPCs for grid cells (above) and non-grid cells (below), for each age. Ages where no data is available is marked with 'N/A'.

5 Discussion

This report has aimed to review some of the standard analysis details of the firing rates of hippocampal cells as an animal moves about an environment. Some analysis on the data of young rats has been made; the number and orientations of maximal Fourier components and the percentage of spatially periodic cells (SPCs) have been considered for each age.

The maximum Fourier components for both grid and non-grid cells followed a trend in their orientation, with peaks about at every 80°. There did seem to be a slight shift to a smaller oscillation period in the grid cells, perhaps being closer to the 60° oscillation reported in other work. It was found that for grid cells the percentage of SPCs increased with age, however in non-grid cells this percentage did not change much with age (furthermore the percentage of SPCs was generally higher for grid cells). This could correspond to the result of Wills *et al* (2010) where certain properties (proportion, stability and quality) of grid cells (unlike place and head-direction) appeared at P20. This suggests that adult-like properties of grid cells develop with age rather than appear from the onset.

Due to the time limitations of this project we were not able to calculate the *number* of Fourier components greater than the 95^{th} percentile of spike shuffled data. It would have been of interest to see if there was any trend with age in the number of main Fourier components in spatially periodic grid and non-grid cells. This could be compared with the results of Krupic *et al* (2012) where grid cells usually had three and non-grid cells had one to four. Also, it would have been more interesting to look at the orientations of components greater than this threshold with age, rather than the method used in this report to find maximal Fourier components used.

Another extension could include looking at spatial periodicity and gridness in the entorhinal cortex and parasubiculum separately. It would interesting to test the suggestion found in Krupic *et al* (2012) that the parasubiculum acts as a sort of stage between periodic bands and stable grids. This could be done by looking at the proportion of SPCs which are grid cells in each of these areas for every age.

In conclusion, trends in the firing properties of hippocampal cells as a rat develops could lead to a better knowledge of which aspects of neural representation exist before experience, and those which emerge with development and/or exploration. This report has attempted to find some of these trends.

Appendix

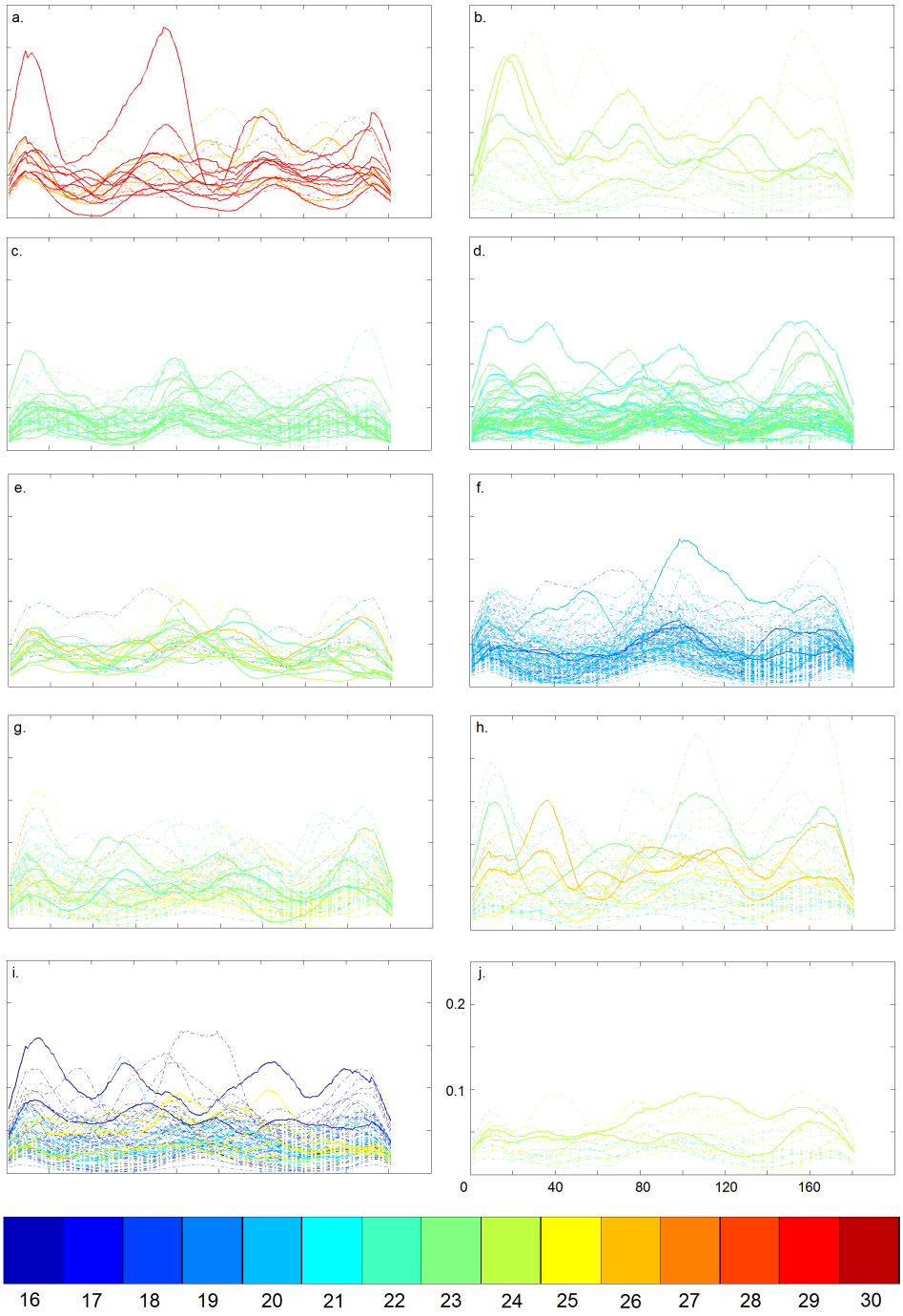

Figure 14: Fourier power plots. Dashed lines represent non-grid cells (gridness scores are less that 0.3), solid lines represent grid cells. Rat 1475 (a), 1493 (b), 1499 (c), 1514 (d), 1547 (e), 1578 (f), 1610 (g), 1612 (h), 1628 (i) and 1630 (j). Age represented by colour (see key).

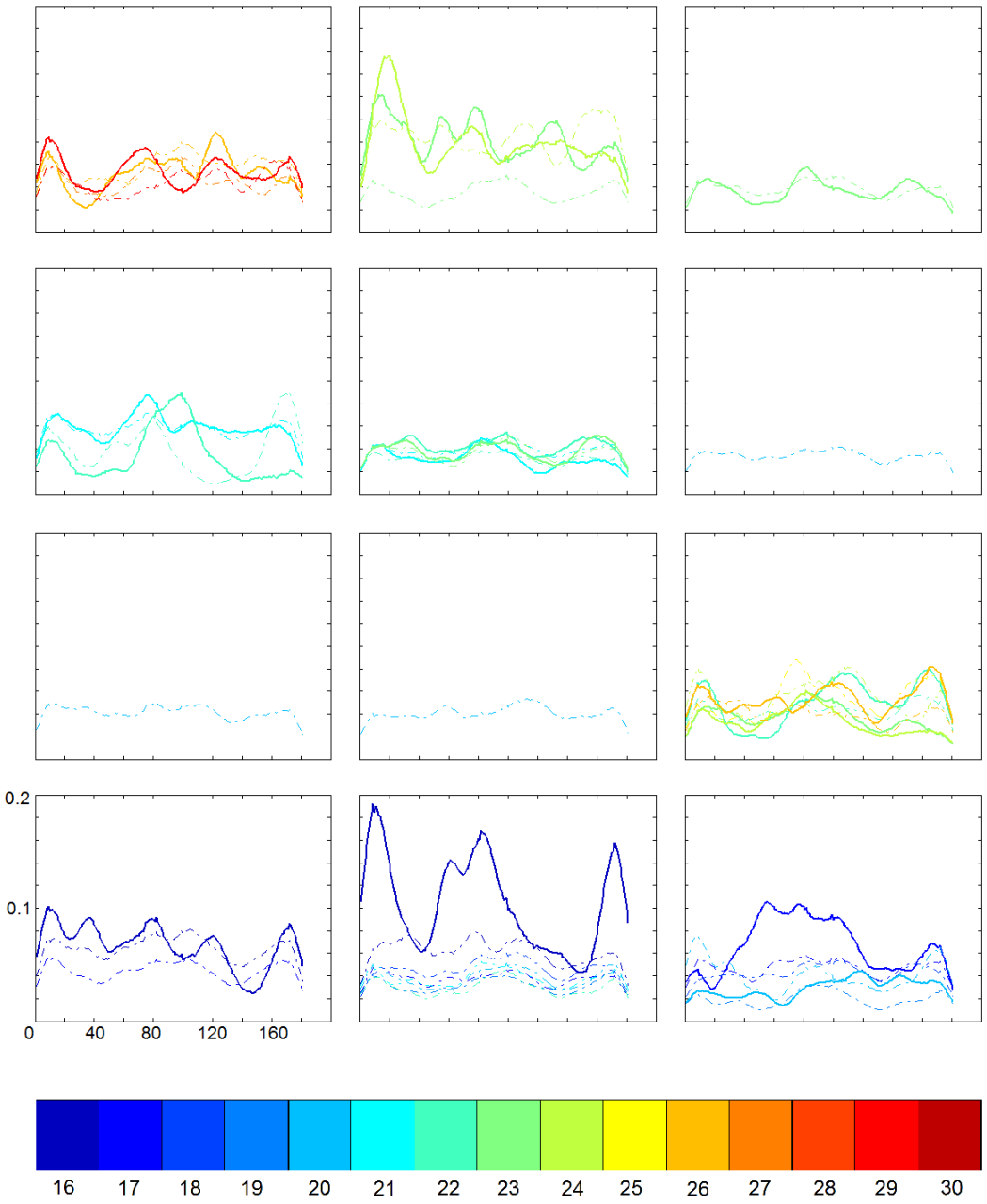

Figure 15: Mean Fourier power for non-grid cells (dashed lines, gridness scores less that 0.3), and grid cells (solid lines). Rats 1475, 1493, 1499, 1500, 1514, 1527, 1528, 1529, 1547, 1551, 1553 and 1555 reading from left to right, top to bottom. Age represented by colour (see key).

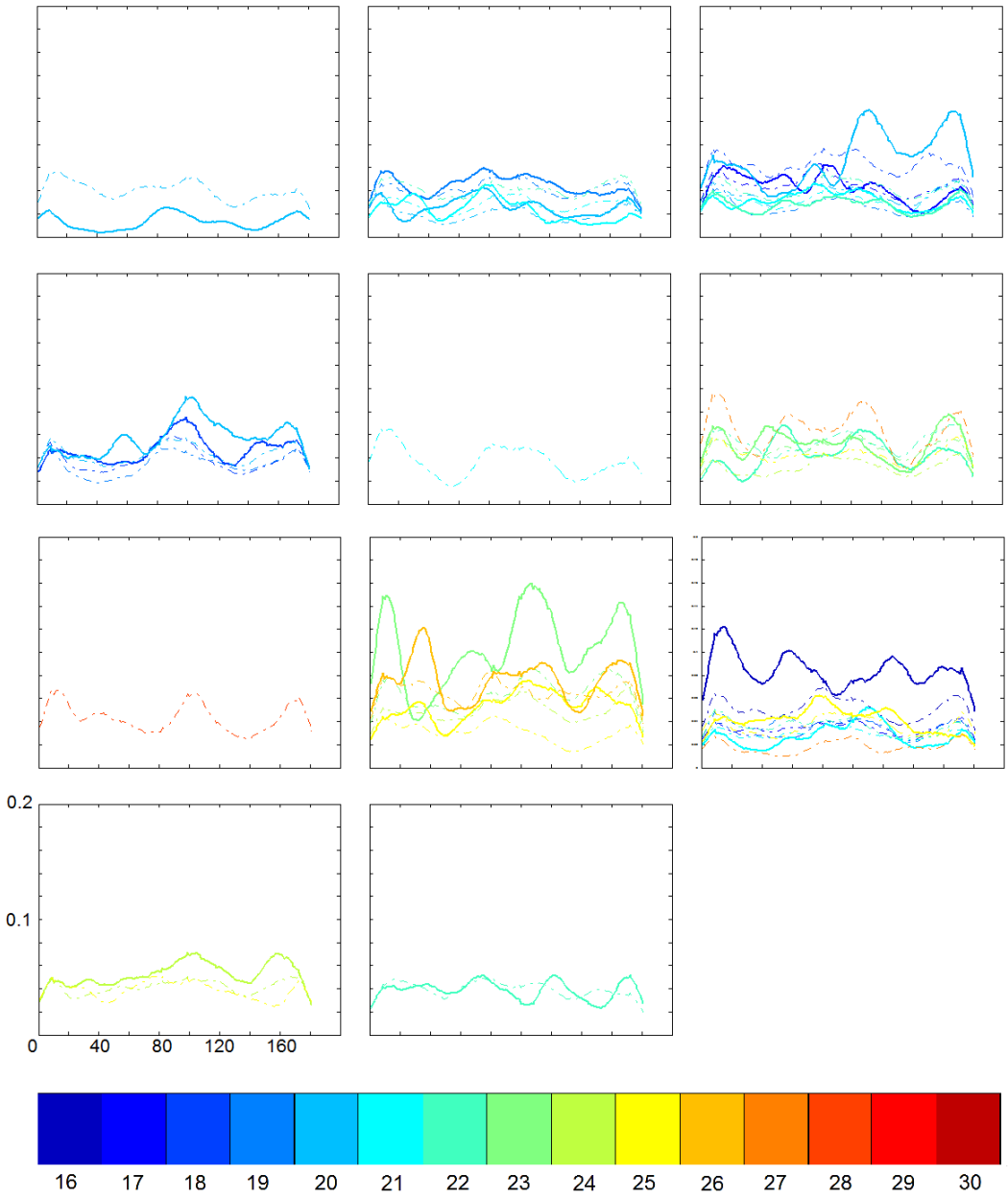

Figure 16: Rats 1563, 1564, 1565, 1578, 1579, 1610, 1611, 1612, 1628, 1630 and 1638.

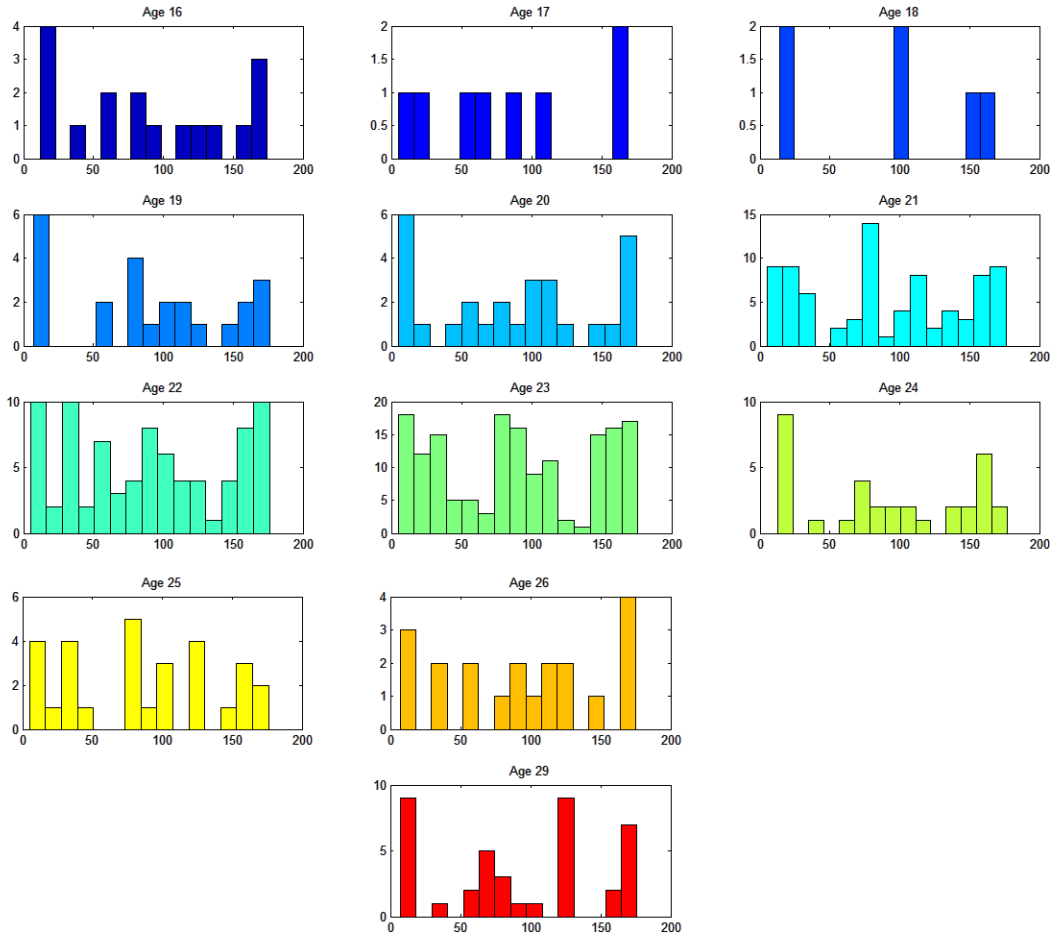

Figure 17: Distribution of maximum Fourier components of grid cells for each age.

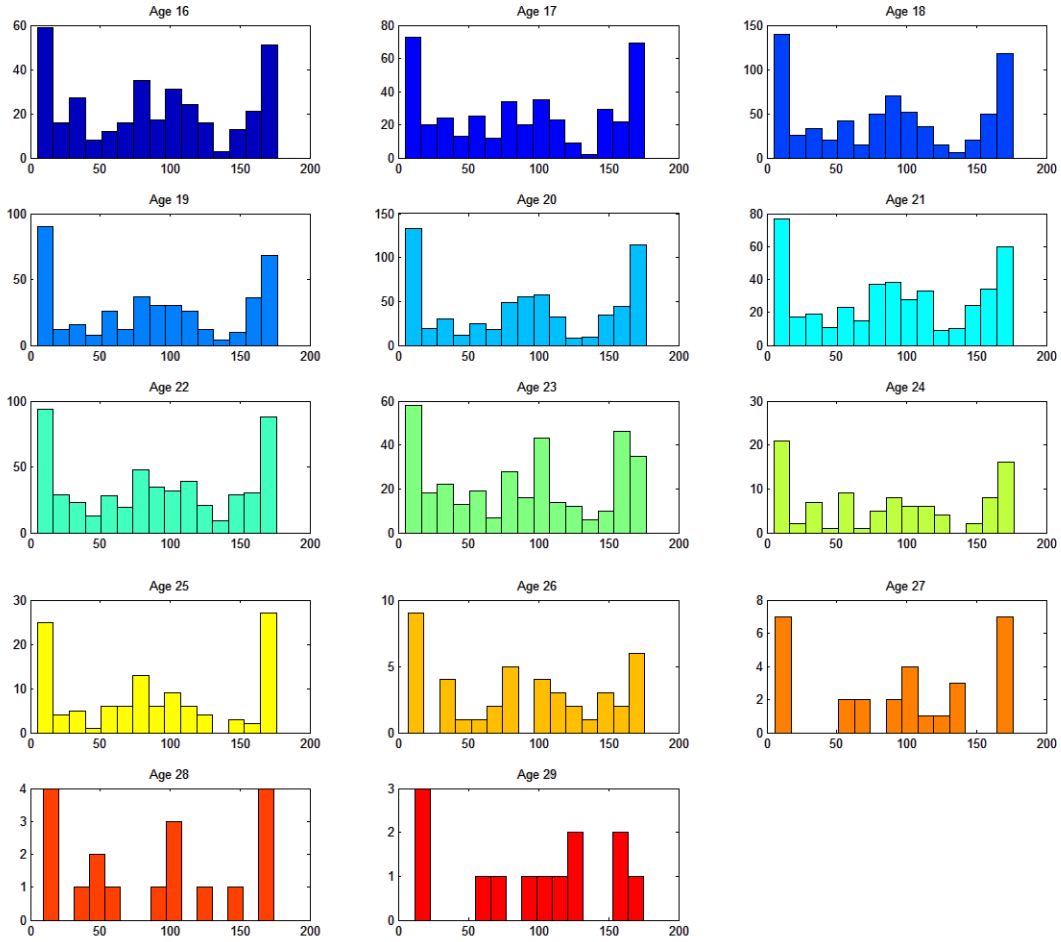

Figure 18: Distribution of maximum Fourier components of non-grid cells for each age.

References

Burgess, N., & O'Keefe, J. 1996. Neuronal computations underlying the firing of place cells and their role in navigation. *Hippocampus* 6 (6): 749-762.

Burgess, N., & OKeefe, J. 2011. Models of place and grid cell firing and theta rhythmicity. *Current opinion in neurobiology* 21 (5): 734-744.

Fyhn, M., Molden, S., Witter, M.P., Moser, E.I. & Moser, M-B. 2004. Spatial representation in the entorhinal cortex. *Science* 305:125864.

Hafting, T., Fyhn, M., Molden, S., Moser, M. B., & Moser, E. I. 2005. Microstructure of a spatial map in the entorhinal cortex. *Nature* 436 (7052): 801-806.

Jeffery, K. J., & Burgess, N. 2006. A metric for the cognitive map: found at last?. *Trends in cognitive sciences* 10 (1): 1-3.

Krupic, J., Burgess, N. & O'Keefe, J. 2012. Neural Representation of Location Composed of Spatially Periodic Bands. *Science* 337 (853): 853-857.

Lever, C., Burton, S., Jeewajee, A., O'Keefe, J., & Burgess, N. 2009. Boundary vector cells in the subiculum of the hippocampal formation. *The Journal of Neuroscience* 29 (31): 9771-9777.

Martin, P. D., & Berthoz, A. 2002. Development of spatial firing in the hippocampus of young rats. *Hippocampus* 12 (4): 465-480.

Moser, E. I., Kropff, E., & Moser, M. B. 2008. Place cells, grid cells, and the brain's spatial representation system. *Annu. Rev. Neurosci.* 31: 69-89.

O'Keefe, J., & Nadel, L. 1978. The hippocampus as a cognitive map. Vol. 3. Oxford: Clarendon Press.

Taube, J. S. 1998. Head direction cells and the neurophysiological basis for a sense of direction. *Progress in neurobiology* 55 (3): 225-256.

Tolman, E. C. (1948). Cognitive maps in rats and men. *Psychological review* 55 (4): 189.

Wills, T., Cacucci, F., Burgess, N. & O'Keefe, J. 2010. Development of the Hippocampal Cognitive Map in Preweanling Rats. *Science* 328 (1573): 1573-1576.